

Phosphorylation of the Budding Yeast 9-1-1 Complex Is Required for Dpb11 Function in the Full Activation of the UV-Induced DNA Damage Checkpoint^{∇†}

Fabio Puddu,[‡] Magda Granata,[‡] Lisa Di Nola,[§] Alessia Balestrini,[¶] Gabriele Piergiovanni, Federico Lazzaro, Michele Giannattasio, Paolo Plevani,^{*} and Marco Muzi-Falconi^{*}

Dipartimento di Scienze Biomolecolari e Biotecnologie, Università degli Studi di Milano, Via Celoria 26, 20133 Milan, Italy

Received 27 February 2008/Returned for modification 26 March 2008/Accepted 27 May 2008

Following genotoxic insults, eukaryotic cells trigger a signal transduction cascade known as the DNA damage checkpoint response, which involves the loading onto DNA of an apical kinase and several downstream factors. Chromatin modifications play an important role in recruiting checkpoint proteins. In budding yeast, methylated H3-K79 is bound by the checkpoint factor Rad9. Loss of Dot1 prevents H3-K79 methylation, leading to a checkpoint defect in the G₁ phase of the cell cycle and to a reduction of checkpoint activation in mitosis, suggesting that another pathway contributes to Rad9 recruitment in M phase. We found that the replication factor Dpb11 is the keystone of this second pathway. *dot1Δ dpb11-1* mutant cells are sensitive to UV or Zeocin treatment and cannot activate Rad53 if irradiated in M phase. Our data suggest that Dpb11 is held in proximity to damaged DNA through an interaction with the phosphorylated 9-1-1 complex, leading to Mec1-dependent phosphorylation of Rad9. Dpb11 is also phosphorylated after DNA damage, and this modification is lost in a nonphosphorylatable *ddc1-T602A* mutant. Finally, we show that, in vivo, Dpb11 cooperates with Dot1 in promoting Rad9 phosphorylation but also contributes to the full activation of Mec1 kinase.

The cellular response to DNA damage is based on signal transduction mechanisms that are essential for the maintenance of genome integrity. The molecules involved and the organization of the pathway are generally conserved in all eukaryotes (2, 29, 30, 42). A major output of this response is a controlled delay in cell cycle progression that regulates the G₁-S transition (G₁ checkpoint) or the G₂-M transition (G₂/M checkpoint; in budding yeast, this response does not regulate the passage from G₂ to M but prevents the anaphase-to-metaphase transition). This is achieved by regulating Cdk kinase or anaphase-promoting complex activities. The current model predicts that genotoxin treatments activate the DNA damage checkpoint response through the recruitment of the ATM and ATR phosphoinositide 3-kinase-related kinases to damaged chromatin (42, 51). The molecular details of the DNA damage signaling pathway in fission and budding yeasts have been mostly worked out by following the phosphorylation of critical kinase substrates in appropriately mutated genetic backgrounds (5, 25). In budding yeast, the prevalent apical kinase is represented by Mec1, which is associated with a Ddc2 subunit. Processing of DNA lesions by repair mechanisms generates

single-stranded DNA (ssDNA) filaments that are rapidly coated by replication protein A (RPA). This structure seems to be responsible for the recruitment of Mec1-Ddc2 (24, 38, 51). The first biochemical event in the signal transduction cascade seems to be the direct phosphorylation of Ddc2 (33, 37). A heterotrimeric complex (9-1-1) composed of Rad17, Mec3, and Ddc1 is loaded onto damaged DNA by a replication factor C-like complex and is itself phosphorylated by Mec1 on the Ddc1 subunit (25, 28, 34). Another Mec1 target is checkpoint factor Rad9, the orthologue of human 53BP1 and fission yeast Crb2. Phosphorylation of Rad9, followed by its oligomerization, allows the recruitment of Rad53 kinase and its activation; it can be visualized as a hyperphosphorylated slower-mobility form by Western blotting (12, 36, 40, 43). Interfering with Rad9 recruitment prevents the activation of Rad53 and cell cycle arrest after DNA damage. Recent work demonstrated that histone H2B ubiquitylation, carried out by Rad6-Bre1, and histone H3 methylation on lysine 79 (H3-K79), performed by Dot1, contribute to Rad9 recruitment to chromatin (11, 13, 14, 48). This pathway depends on an interaction between methylated H3-K79 and the Tudor domain of Rad9. Loss of these histone modifications (e.g., in *dot1Δ* mutant cells) or mutation of the Rad9 Tudor domain prevents Rad9 and Rad53 phosphorylation in G₁-arrested cells and abolishes the G₁-S arrest following DNA damage (11, 13, 48). The current model predicts that Rad9 bound to histone H3 can be phosphorylated by Mec1 and then binds to phosphorylated H2A (14). Surprisingly, in M cells, deletion of *DOT1* is not sufficient to eliminate checkpoint function. *dot1Δ* mutant cells are not particularly sensitive to Zeocin or UV and, when irradiated in M, display an apparently normal cell cycle arrest, despite a lower level of Rad53 phosphorylation, mirrored by a slightly reduced modification of Rad9 (11). These observations suggest that the

* Corresponding author. Mailing address: Dipartimento di Scienze Biomolecolari e Biotecnologie, Università degli Studi di Milano, Via Celoria 26, 20133 Milan, Italy. Phone for Marco Muzi-Falconi: 39 02 50315034. Fax: 39 02 50315044. E-mail: marco.muzifalconi@unimi.it. Phone for Paolo Plevani: 39 02 50315032. Fax: 39 02 50315044. E-mail: paolo.plevani@unimi.it.

† Supplemental material for this article may be found at <http://mcb.asm.org/>.

‡ These authors contributed equally to this work.

§ Present address: Teva Pharma Italia, Milan, Italy.

¶ Present address: Genome Stability Unit, Clare Hall Laboratories, London Research Institute, London, United Kingdom.

[∇] Published ahead of print on 9 June 2008.

pathways involved in the recruitment of Rad9 to chromatin are somehow cell cycle specific; in M cells, another mechanism, partially redundant with the histone modification pathway, must be active to obtain Rad9 phosphorylation and effective checkpoint activation. In the last few years, results obtained with fission yeast, *Xenopus laevis* extracts, and human cells revealed that a new player involved in the DNA damage response is a factor called Rad4/Cut5 in *Schizosaccharomyces pombe*, TopBP1 in higher eukaryotes, and Dpb11 in budding yeast (6–8, 21, 35). These proteins share the presence of BRCT domains, which are involved in protein-protein interactions. The general picture that is starting to emerge is that this factor interacts with phosphoinositide 3-kinase-related kinases, possibly controlling their activity; it is recruited to DNA by interacting with the 9-1-1 complex and facilitates downstream signaling by interacting with Crb2/53BP1 (3, 9). The role played by Dpb11 in the DNA damage response in budding yeast has not been described, and here we show that it is an essential component of this new G₂/M pathway which allows Rad9 recruitment and checkpoint activation in the absence of histone H3 methylation. We provide evidence suggesting that, in M-phase cells, Rad9 can be phosphorylated by Mec1 through H3-K79 methylation or through an interaction with Dpb11. We also show that the functional interaction between Dpb11 and the Ddc1 subunit of the 9-1-1 complex is regulated by a Mec1-dependent phosphorylation of a specific Ddc1 C-terminal threonine, which likely allows the recruitment of Dpb11 to damaged chromatin and its phosphorylation by Mec1. Finally, we provide in vivo evidence that in budding yeast, Dpb11 is involved in directly regulating the apical kinase Mec1.

MATERIALS AND METHODS

Strains and plasmids. All of the strains used in this work are derivatives of W303 (K699 [*MATa ade2-1 trp1-1 can1-100 leu2-3,12 his3-11,15 ura3*]), except histone H4 mutants. The K20R and K59R histone H4 mutants were obtained by plasmid shuffling with pFL17.5 and pFL19.5, respectively, in strain UCC1111 (20). These last plasmids were obtained by PCR over pMP3 (20) with mutagenic oligonucleotides.

The YFP20 (*dpb11-1*) and YMAG6 (*dpb11-1dot1Δ*) strains were obtained by PstI-directed integration of YIplac211-*dpb11-1* (1) into K699 and YFL234, respectively (11). Plasmid pop-out events were selected on 5-fluoroorotic acid plates, and the presence of the *dpb11-1* allele was confirmed by checking the temperature-sensitive phenotype and by PCR analysis to confirm the presence of the mutation. All of the other *DPB11* mutant strains were obtained by crossing; myc-tagged *DPB11* mutant strains were obtained by using the one-step PCR system (27) to allow detection by Western blotting; however, tagged Dpb11 cannot be immunoprecipitated, likely because the tag is hidden in the native protein.

DDC1 site-specific mutations were obtained by PCR with mutagenic oligonucleotides by using the pML89 plasmid (26). Multiple round of mutagenesis over these plasmids allowed the construction of the pLD12, pLD26, and pLD31 plasmids, carrying the *ddc1-M3* (S413A, S436A, T444A), *ddc1-M8* (T342A, S469A, S471A, S495A, T529A, S532A, S580A, T602A), and *ddc1-M11* (containing a combination of all of the above-mentioned point mutations) alleles, respectively. All of these plasmids were transformed into *ddc1Δ* mutant strain YLL244 (26) to obtain *ddc1* mutant yeast strains. Plasmid pFP9 carrying the *ddc1-T602S* mutation was obtained by PCR with mutagenic oligonucleotides by using the pML89 plasmid as the template.

Strains carrying a Dpb11 degron tag, YJT70 (*dpb11^{td}*) and Y1812 (*dpb11^{td} DPB11*), were a kind gift from J. F. X. Diffley.

All of the strains used in this study are described in Table 1.

DNA damage sensitivity assay. In order to assess cell survival after UV irradiation, yeast strains were cultured overnight to stationary phase. Cells were then diluted, and approximately 200 cells were plated on petri dishes, which were irradiated with different UV doses. After 3 days, the total number of colonies

that formed on each plate was determined. Alternatively, overnight cultures were diluted to 1×10^6 cells/ml and then 10-fold serial dilutions were prepared and 10- μ l volumes of the suspensions were spotted onto plates, which were either UV irradiated or mock treated. To assess survival of Zeocin treatment, exponentially growing cells were treated for 30 min with different concentrations of the drug. After Zeocin removal, cultures were diluted to 1×10^6 cells/ml and then 10-fold serial dilutions were prepared and 10- μ l volumes of the suspensions were spotted onto YPD plates (31). Images were taken 3 days later.

SDS-PAGE and Western blotting. Protein extracts obtained with trichloroacetic acid (31) were separated by sodium dodecyl sulfate-polyacrylamide gel electrophoresis (SDS-PAGE) in 10% acrylamide gels; for analysis of Rad9 phosphorylation, NuPAGE Tris-acetate 3 to 8% gels were used by following the manufacturer's instructions. Western blotting was performed with anti-Rad53, anti-myc (9E10), antihemagglutinin (anti-HA; 12CA5), anti-Ddc1, and anti-Rad9 antibodies by using standard techniques. For more efficient detection of phosphorylated Dpb11 isoforms, 7.5% acrylamide gels supplemented with Phos tag-conjugated acrylamide were used according to the manufacturer's instructions (NARD Institute Ltd.).

Cell cycle blocks and DNA damage treatment. Cells were grown in YPD medium at 28°C (25°C in the experiments with strains harboring the *dpb11-1* mutation) to a concentration of 5×10^6 /ml and arrested with nocodazole (20 μ g/ml). Fifty-milliliter volumes of cultures were spun, resuspended in 500 μ l of fresh YPD plus nocodazole, and plated on a petri dish (14-cm diameter). Plates were quickly irradiated at 75 J/m², and cells were resuspended in 50 ml of YPD plus nocodazole. A 25-ml sample was taken immediately and processed for protein extract preparation, while a second 25-ml sample was taken 30 min afterward. For analysis of the double-strand break (DSB) checkpoint response, nocodazole-arrested cells were treated with 100 μ g/ml Zeocin. Samples were taken from the culture every 15 min and processed for protein extraction.

G₂/M checkpoint assay. Yeast cells were synchronized in M by treating exponentially growing cultures with 5 μ g/ml nocodazole. UV treatment was performed as described previously (10), except that 6 μ g/ml α -factor was added to the resuspension medium. Cells were then stained with 4',6'-diamidino-2-phenylindole (DAPI), and nuclear division was monitored by microscopic analysis.

Use of the *dpb11^{td}* allele. As previously described (44, 49), the *dpb11^{td}* mutant strain (YJT70) contains the Dpb11-td fusion under the control of tTA and the *tetO2* promoter, the E3 ubiquitin ligase gene *UBR1* under the control of the inducible *GAL1* promoter, and three copies of pCM244 harboring a mutated Tet repressor-SSN6 fusion (*tetR'-SSN6*) gene integrated at the *LEU2* locus. Y1812 (*dpb11^{td} DPB11*) is isogenic to strain YJT70, but it also contains a copy of the *DPB11* gene under the control of its own promoter. YMAG78/4b and YMAG82/15a are derivatives of YJT70 and Y1812, respectively, carrying an HA-tagged version of Ddc2.

These strains were grown in YP plus raffinose at 28°C to a concentration of 5×10^6 cells/ml and arrested with nocodazole. Twenty-five milliliters of arrested cells was immediately processed for protein extraction with trichloroacetic acid. The rest of the culture was shifted to 37°C in the presence of galactose (2%) and tetracycline (50 μ g/ml) for 2.5 h. This treatment leads to Dpb11-td degradation and represses *dpb11^{td}* transcription, inducing the *dpb11*-encoded phenotype. A 150-ml volume of cells was spun, resuspended in 1.5 ml of the same medium, and UV irradiated as described previously. After treatment, cultures were shifted to 28°C. A 25-ml sample was taken immediately and processed for protein extract preparation, and a second 25-ml sample was taken 30 min later.

RESULTS

We have previously shown that ubiquitylation of histone H2B by the Rad6/Bre1 complex and methylation of histone H3 on the K79 residue, mediated by Dot1, are prerequisites for a functional response to DNA damage in the G₁ phase of the *Saccharomyces cerevisiae* cell cycle (11). This requirement seems to be ascribed to the capacity of the Rad9 checkpoint protein to bind methylated H3-K79 through its Tudor domain. In fact, in the absence of H3-K79 methylation or if the Rad9 Tudor domain is mutated, yeast cells damaged in G₁ do not exhibit Rad9 loading onto DNA and are deficient in transmitting the checkpoint signal from the ATR-like kinase Mec1 to the Chk2-like kinase Rad53 (11, 13, 14, 18, 48). Surprisingly, if *dot1Δ* mutant cells are treated with Zeocin or UV light in the

TABLE 1. Strains used in this study

Strain	Relevant genotype	Source
K699	<i>MATa ade2-1 trp1-1 leu2-3,112 his3-11,15 ura3 can1-100</i>	K. Nasmyth
K700	<i>MATα ade2-1 trp1-1 leu2-3,112 his3-11,15 ura3 can1-100</i>	K. Nasmyth
YFL448/1a	K700 <i>dot1::kanMX6 tel1::HIS3</i>	This work
YFL438	K699 <i>dot1::kanMX6 mec1-1 sml1</i>	This work
YFL499/3d	K699 <i>dot1::kanMX6 chk1::kanMX6</i>	This work
YFL224	K699 <i>bre1::kanMX6</i>	M. Giannattasio
YFL236	K699 <i>set2::kanMX6</i>	This work
YMG203	K699 <i>bre1::kanMX6 set2::kanMX6</i>	This work
UCC1111	<i>MATα ade2::his3Δ200 leu2Δ0 lys2Δ0 met15Δ trp1Δ63 ura3Δ0 adh4::URA3-TEL (VII-L) hhf2-hht2::MET15 hhf1-hht1::LEU2(pRS412-ADE2 CEN ARS-HHF2-HHT2)</i>	D. E. Gottschling
YFL287	UCC1111(pMP3)	This work
YFL288	UCC1111(pFL17.5 [H4-K20R])	This work
YFL290	UCC1111(pFL19.5 [H4-K59R])	This work
YFL292	UCC1111 <i>dot1::kanMX6</i> (pMP3)	This work
YFL294	UCC1111 <i>dot1::kanMX6</i> (pFL17.5 [H4-K20R])	This work
YFL296	UCC1111 <i>dot1::kanMX6</i> (pFL19.5 [H4-K59R])	This work
YFP20	K699 <i>dpb11-1</i>	This work
YFL234	K699 <i>dot1::kanMX6</i>	M. Giannattasio
YMAG6	K699 <i>dot1::kanMX6 dpb11-1</i>	This work
YMIC4F6	K699 <i>mec3::TRP1 rad9::URA3</i>	This work
YLL683.8/3B	K699 <i>ddc2::DDC2-3HA:URA3</i>	M. P. Longhese
YFP24/6b	K699 <i>dpb11-1 ddc2::DDC2-3HA:URA3</i>	This work
YFL403/10b	K699 <i>dot1::kanMX6 ddc2::DDC2-3HA:URA3</i>	F. Lazzaro
YFL687/2b	K699 <i>dot1::kanMX6 dpb11-1 ddc2::DDC2-3HA:URA3</i>	This work
YFL211/3a	K699 <i>RAD9-13myc:TRP1 ddc1::DDC1-HA:LEU2</i>	This work
YMAG48/5b	K700 <i>dpb11-1 RAD9-13myc:TRP1 ddc1::DDC1-HA:LEU2</i>	This work
YMAG34/4a	K699 <i>dot1::kanMX6 RAD9-13myc:TRP1 ddc1::DDC1-HA:LEU2</i>	This work
YMAG52/3d	K699 <i>dot1::kanMX6 dpb11-1 RAD9-13myc:TRP1 ddc1::DDC1-HA:LEU2</i>	This work
YMIC4E8	K699 <i>rad9::URA3</i>	F. Lazzaro
YMAG149/7B	K699 <i>hta1-htb1::LEU2 hta2-htb2::TRP1</i> (pSAB6 [HTA1-HTB1])	This work
YMAG168	K699 <i>hta1-htb1::LEU2 hta2-htb2::TRP1</i> (pJD151 [hta1-S129A-HTB1])	This work
YMAG150/4A	K699 <i>dot1::kanMX6 hta1-htb1::LEU2 hta2-htb2::TRP1</i> (pSAB6 [HTA1-HTB1])	This work
YMAG170	K699 <i>dot1::kanMX6 hta1-htb1::LEU2 hta2-htb2::TRP1</i> (pJD151 [hta1-S129A-HTB1])	This work
YLDN25	K699 <i>ddc1::kanMX4</i> (pML89)	This work
YLDN17	K699 <i>ddc1::kanMX4</i> (pLD12)	This work
YLDN23	K699 <i>ddc1::kanMX4</i> (pLD26)	This work
YLDN24	K699 <i>ddc1::kanMX4</i> (pLD31)	This work
YFP27	K699 <i>ddc1::kanMX4 dot1::HIS3</i> (pML89)	This work
YFP28	K699 <i>ddc1::kanMX4 dot1::HIS3</i> (pLD12)	This work
YFP29	K699 <i>ddc1::kanMX4 dot1::HIS3</i> (pLD26)	This work
YFP30	K699 <i>ddc1::kanMX4 dot1::HIS3</i> (pLD31)	This work
YLDN9	K699 <i>ddc1::kanMX4</i> (pLD9)	This work
YFP37	K699 <i>ddc1::kanMX4 dot1::HIS3</i> (pLD9)	This work
YFP148	K699 <i>ddc1::kanMX6</i> (pFP9)	This work
YFP149	K699 <i>ddc1::kanMX6 dot1::HIS3</i> (pFP9)	This work
YFP38	K699 <i>dpb11::DPB11-13myc:HIS3</i>	This work
YFP48/3a	K699 <i>dpb11::DPB11-13myc:HIS3 mec1-1 sml1-1</i>	This work
YFP49/1d	K699 <i>dpb11::DPB11-13myc:HIS3 rad53::kanMX6 sml1::HIS3</i>	This work
YFP55/6c	K699 <i>ddc1::kanMX6 dpb11::DPB11-13myc:HIS3</i>	This work
YFP56	K699 <i>ddc1::kanMX6 dpb11::DPB11-13myc:HIS3</i> (pML89)	This work
YFP57	K699 <i>ddc1::kanMX6 dpb11::DPB11-13myc:HIS3</i> (pLD9)	This work
YFP63	K699 <i>ddc1::kanMX6</i> (pML89)	This work
YFP64	K699 <i>ddc1::kanMX6</i> (pLD9)	This work
YFP65	K699 <i>ddc1::kanMX6 dpb11-1</i> (pML89)	This work
YFP66	K699 <i>ddc1::kanMX6 dpb11-1</i> (pLD9)	This work
YFP 152	K699 <i>ddc1::kanMX6</i> [Ycplac111]	This work
YFP 142	K699 <i>dot1::HIS3 dpb11-1 ddc1::kanMX6</i> (pML89)	This work
YFP 144	K699 <i>dot1::HIS3 dpb11-1 ddc1::kanMX6</i> (pLD9)	This work
YFP50	EGY48(pSH18.34/pFP1/pFP2)	This work
YFP52	EGY48(pSH18.34/pFP1/pFP4)	This work
YFP113	K699 <i>mec1-1 sml1</i> (pSH18.34/pFP1/pFP2)	This work
YFP114	K699 <i>mec1-1 sml1</i> (pSH18.34/pFP1/pFP4)	This work
YFP86	EGY48(pSH18.34/pJG4-5/pFP2)	This work
YFP54	EGY48(pSH18.34/pFP1/pEG202)	This work
YFP153	EGY48(pSH18.34/pFP1/pFP10)	This work
YMAG78/4b	Y1812 <i>ddc2HA-URA3</i>	This work
YMAG82/15a	YJT70 <i>ddc2HA-URA3</i>	This work

M phase of the cell cycle, residual phosphorylation of Rad53 can be observed and the G₂/M checkpoint response is partially proficient, allowing *dot1Δ* mutant cells to survive the treatment (11). This finding suggests that a different mechanism of Rad9 recruitment can compensate for the loss of H3-K79 methylation in M cells.

To define the nature of this second pathway, active in the M phase of the cell cycle, we first verified whether the activation of Rad53 observed in the absence of H3-K79 methylation (i.e., *dot1Δ* mutant cells) was due to the unscheduled activation of a pathway dependent upon the apical kinase Tel1 and/or Chk1. *dot1Δ*, *dot1Δ tel1Δ*, *dot1Δ chk1Δ*, and *dot1Δ mecl1-1* mutant cells were arrested with nocodazole and UV irradiated to trigger the DNA damage checkpoint. Phosphorylation of Rad53 was evaluated as a mobility shift of Rad53 on SDS-PAGE. Cells with a *DOT1* deletion still exhibit significant Rad53 phosphorylation when irradiated in the M phase of the cell cycle; deletion of *TEL1* or *CHK1* does not affect this residual Rad53 phosphorylation, which is instead abolished in a *mecl1-1* background (see Fig. S1A in the supplemental material; data not shown).

Rad53 phosphorylation correlates with Rad9 phosphorylation also in the absence of methylated H3-K79 (11); we thus tested whether other histone modifications known to be somehow involved in the DNA damage response might be redundant with H3-K79 methylation and cooperate in Rad9 recruitment. The Set1 and Set2 histone methyltransferases are required for H3-K4 and H3-K36 methylation, respectively (22). Moreover, Set1 has been suggested to play a partial role in the intra-S DNA damage checkpoint (11). Abolishing the function of Set1 and Set2 did not affect Rad53 phosphorylation in wild-type (WT) cells, nor did it reduce the residual Rad53 activation detected when *dot1Δ* mutant cells were UV irradiated in M phase (see Fig. S1B in the supplemental material) (13). In the structure of the nucleosome, H3-K79 is very close to H4-K59 (50), and in *S. pombe*, methylated H4-K20 binds Crb2, the Rad9 orthologue (39). We thus tested the contribution of these residues by analyzing Rad53 phosphorylation in cells carrying H4-K20R or H4-K59R mutations in a *dot1Δ* mutant background. When these strains were treated with UV in M phase, they displayed the same level of Rad53 phosphorylation as the isogenic *dot1Δ* mutant cells (see Fig. S1C in the supplemental material); similar results were obtained when the deletion of *DOT1* was combined with a point mutation in the histone H2A tail, preventing the damaged-induced phosphorylation of serine 129 (see Fig. S1D in the supplemental material). These observations suggested the existence of a different, histone-independent, pathway involved in Rad9 recruitment.

In *S. pombe*, Crb2 can be recruited to chromatin through an interaction with Cut5/Rad4 to fulfill its function in the checkpoint response (7). We analyzed whether Dpb11, the budding yeast orthologue of Cut5/Rad4, might be involved in recruiting Rad9 to chromatin and possibly be responsible for the activation of Rad53 observed in UV-irradiated *dot1Δ* mutant M-phase cells.

In order to address this question, we generated strains carrying a temperature-sensitive *dpb11-1* mutation in a *dot1Δ* mutant background and monitored the cellular response to UV. The *dpb11-1* mutant at permissive temperature grows normally (1). Under our experimental conditions, when ex-

posed to different levels of UV light, the *dpb11-1* and *dot1Δ* mutant strains are slightly more sensitive than WT cells. Interestingly, the *dot1Δ* and *dpb11-1* mutations exhibit synergistic effects on sensitivity to UV; indeed, the *dot1Δ dpb11-1* double mutant is noticeably more sensitive than either one of the single mutants and closely resembles a *rad9Δ* mutant strain (Fig. 1A). In order to test their capacity to delay cell cycle progression following UV irradiation, the WT and mutant strains were arrested with nocodazole, treated with UV light, and released into the cell cycle. Nuclear division was monitored by DAPI staining and microscopic analysis. As shown in Fig. 1B, UV-treated *dpb11-1* and *dot1Δ* mutant cells exhibit a nuclear division profile which is very similar to the profile of a WT strain, suggesting an almost normal checkpoint response after UV damage. On the other hand, the double mutant completely loses the delay and behaves almost identically to *mec3Δ rad9Δ* mutant, checkpoint-null control cells.

We then analyzed the phosphorylation cascade that is triggered by UV, monitoring the phosphorylation state of the Ddc2, Rad9, and Rad53 factors, which act sequentially in the checkpoint cascade. Figure 1C shows that in M phase, *dot1Δ* mutant cells partially maintain the capacity to activate the checkpoint after UV irradiation and to significantly phosphorylate both Rad9 and Rad53. This residual response to UV damage, observed in the absence of H3-K79 methylation, is dependent upon *DPB11*. Indeed, Rad9 and Rad53 do not exhibit any DNA damage-induced modification in the *dot1Δ dpb11-1* double mutant, while Mec1 activity, as measured by Ddc2 phosphorylation, does not seem to be significantly reduced. The data described so far indicate that the role of *DPB11* in this pathway is to facilitate Rad9 phosphorylation, possibly by providing an alternative way for its recruitment to chromatin, suggesting that *DPB11* and *DOT1* may be working in two parallel pathways leading to Rad9 and Rad53 phosphorylation. If UV irradiated in G₁, *dot1Δ* mutant cells are unable to delay entry into S phase and budding, and Rad53 phosphorylation is grossly defective (11). Under these conditions, a minor phosphorylation of Rad53 can be detected in *dot1Δ* mutant cells only if cultures are held in G₁ for at least 30 min after the genotoxic treatment, and this residual checkpoint activity is *DPB11* dependent, being lost in *dot1Δ dpb11-1* mutant cells (Fig. 1D).

We then analyzed whether this mechanism is UV specific or is also involved in the response to DSBs. Nocodazole-arrested cells were treated with the DSB-inducing agent Zeocin; survival and Rad53 activation were then monitored in WT and *dot1Δ*, *dpb11-1*, and *dot1Δ dpb11-1* mutant cells. Even in response to DSBs, a mutation in *DPB11* is synthetic with the loss of H3-K79 methylation; in fact, the *dot1Δ dpb11-1* double mutant is more sensitive than either single mutant (Fig. 2A) and Rad53 phosphorylation is grossly defective in double-mutant cells (Fig. 2B).

Previously published evidence indicates that Dpb11 interacts physically and genetically with the Ddc1 subunit of the 9-1-1 checkpoint clamp; this interaction seems to involve the last BRCT domain of Dpb11, which is a phosphoprotein binding motif (47). Since Ddc1 is subject to cell cycle-dependent and DNA damage-dependent phosphorylation (26, 34), we tested whether Ddc1 phosphorylation plays any role in controlling this Dpb11-dependent pathway. The deduced protein se-

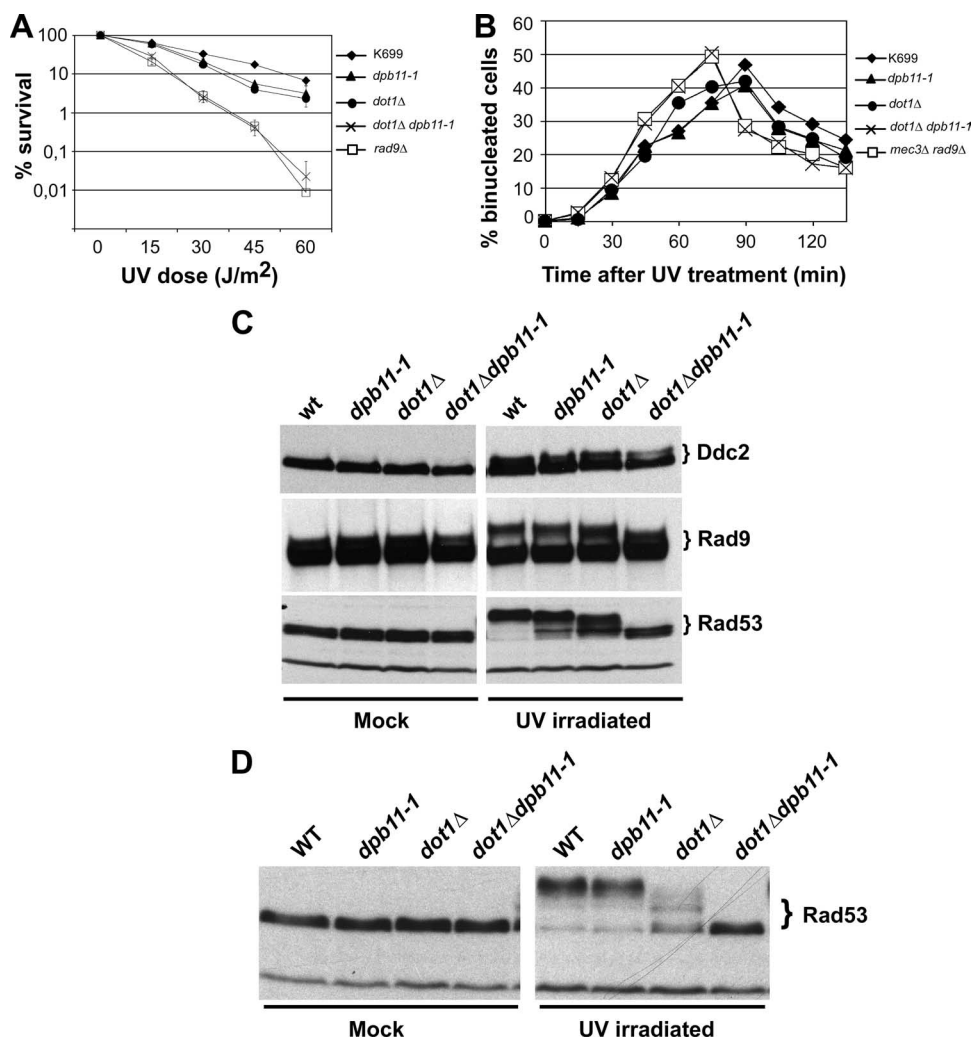


FIG. 1. Dpb11 function is required for the Dot1-independent checkpoint activation pathway in response to UV irradiation. (A) UV survival assay. Strains K699 (WT), YMIC4E8 (*rad9Δ*), YFP20 (*dpb11-1*), YFL234 (*dot1Δ*), and YMAG6 (*dot1Δ dpb11-1*) were grown overnight to stationary phase and then diluted and plated on YPD plates, which were irradiated with the indicated UV doses. Survival was assayed by determining the number of colonies that formed on the plates after 3 days. (B) UV checkpoint assay. Yeast strains K699 (WT), YFP20 (*dpb11-1*), YFL234 (*dot1Δ*), YMAG6 (*dot1Δ dpb11-1*), and YMIC4F6 (*mec3Δ rad9Δ*) were synchronized in M phase with nocodazole, UV irradiated at 40 J/m², and released in YPD plus α -factor. Every 15 min, samples were taken and scored for the presence of binucleated cells. (C) Analysis of the phosphorylation of checkpoint factors. WT and *dpb11-1*, *dot1Δ*, and *dot1Δ dpb11-1* mutant cells carrying Ddc2-HA and Rad9-myc were arrested with nocodazole and either mock or UV irradiated (75 J/m²); 30 min after irradiation, Ddc2, Rad9, and Rad53 phosphorylations were analyzed by SDS-PAGE and Western blotting. (D) Strain K699 (WT), YFP20 (*dpb11-1*), YFL234 (*dot1Δ*), and YMAG6 (*dot1Δ dpb11-1*) cells were cultured to mid-log phase, arrested in G₁ with 20 μ g/ml α -factor, and either mock or UV irradiated (75 J/m²); 30 min after irradiation, Rad53 phosphorylation was analyzed by SDS-PAGE and Western blotting.

quence of Ddc1 reveals the presence of three consensus phosphorylation sites for cyclin-dependent kinases and eight putative target sites for Mec1. By site-specific mutagenesis, we converted the phosphorylatable residues to alanine and constructed the *ddc1-M3* allele, lacking the putative Cdk target sites; the *ddc1-M8* allele, lacking the Mec1 target sites; and the *ddc1-M11* allele, lacking all sites (Fig. 3A). In order to determine the contribution of these phosphorylation sites to DNA damage-induced Ddc1 phosphorylation, the phosphorylation state of these mutant proteins was tested after treatment with UV light. While mutations of the Cdk consensus sites do not affect the UV-induced phosphorylation of Ddc1, the damage-dependent mobility shift of Ddc1 is lost in *ddc1-M8* and *ddc1-*

M11 mutant strains (Fig. 3B). The role of these phosphorylation sites in the downstream events in the DNA damage checkpoint cascade was further investigated by analyzing the effects of the *ddc1-M3*, *ddc1-M8*, and *ddc1-M11* mutations on Rad9 and Rad53 phosphorylation after UV irradiation in nocodazole-arrested cells. Our results show that none of the *DDC1* phosphorylation mutant alleles affects the checkpoint response when H3-K79 can be methylated. On the other hand, both *ddc1-M8* and *ddc1-M11* produce a synthetic phenotype when combined with a *dot1Δ* mutation; both *ddc1-M8 dot1Δ* and *ddc1-M11 dot1Δ* mutant strains lose the ability to hyperphosphorylate Rad9 and Rad53 (Fig. 4A and data not shown) and acquire a UV hypersensitivity similarly to what we ob-

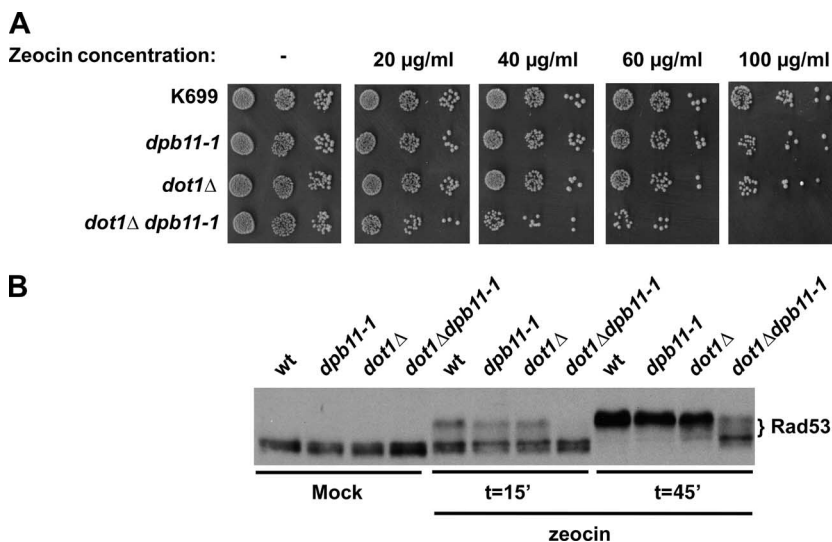


FIG. 2. Dpb11 and Dot1 cooperate in the checkpoint activation pathway in response to DSB-inducing agents. (A) DSB survival assay. Strains K699 (WT), YFP20 (*dpb11-1*), YFL234 (*dot1Δ*), and YMAG6 (*dot1Δ dpb11-1*) were grown to mid-log phase and then treated for 30 min with Zeocin at the indicated concentrations. Serial dilutions were then spotted onto YPD plates and incubated for 3 days. (B) Analysis of checkpoint activation after treatment with DSB-inducing agents. Strains K699 (WT), YFP20 (*dpb11-1*), YFL234 (*dot1Δ*), and YMAG6 (*dot1Δ dpb11-1*) were cultured to mid-log phase and either mock treated or treated with 100 μg/ml Zeocin. At 15 and 45 min after drug addition, samples were taken and processed for the analysis of Rad53 phosphorylation.

served in *dot1Δ dpb11-1* mutant cells (Fig. 4B and data not shown). Such observations suggest that a pathway requiring Dpb11 and Mec1-dependent phosphorylation of Ddc1 collaborates with methylated H3-K79 in checkpoint activation and is required to phosphorylate Rad9 in the absence of the histone-mediated pathway. These results are in agreement with data obtained in other eukaryotic systems showing that the interaction of TopBP1 and Cut5 with the 9-1-1 complex requires the phosphorylation of the Ddc1 orthologues (6, 8, 23).

In order to gain more insight into the mechanism of this pathway, we investigated the individual roles of the putative Mec1-dependent phosphorylation sites by testing the effect

of the mutation of each site on the activation of Rad9. For this purpose, we combined *dot1Δ* with *ddc1* alleles carrying different serine/threonine-to-alanine point mutations in each of the eight Mec1 target sites and monitored the activation of Rad53 and the phosphorylation of Rad9 after UV irradiation. With this analysis, we determined that T602 is the critical residue for the function of this pathway. In fact, Fig. 5A shows that *ddc1-T602A* has the same synthetic effect, in combination with *dot1Δ*, as the one displayed by *ddc1-M8*; this is the only mutation, of the eight that were tested, which was able to abolish the residual Rad53 phosphorylation and to prevent Rad9 phosphorylation in a *dot1Δ*

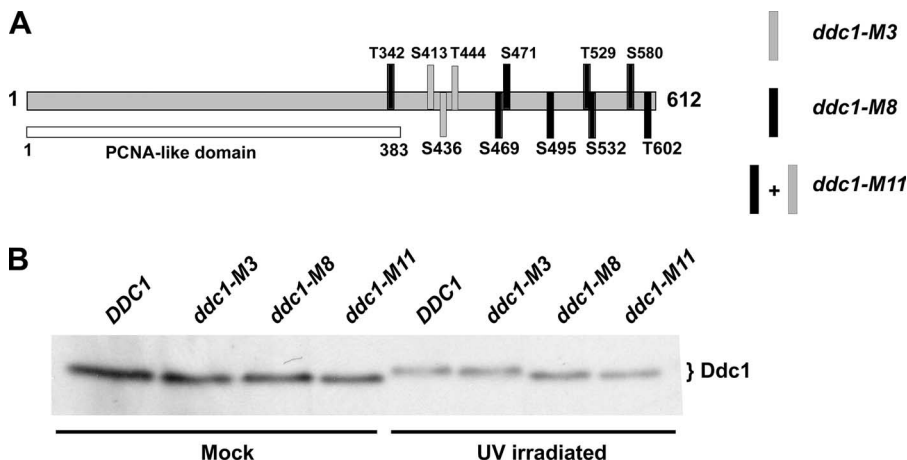


FIG. 3. UV-induced Ddc1 phosphorylation depends upon the presence of Mec1 kinase consensus sites. (A) Outline of the Cdc28 (gray) and Mec1 (black) putative phosphorylation target sites in Ddc1. Cdc28 and Mec1 target sites were mutated to alanine in *ddc1-M3* and *ddc1-M8* mutant strains, respectively. The *ddc1-M11* mutant strain contains a combination of all of these mutations. (B) Strains YLDN25 (WT), YLDN17 (*ddc1-M3*), YLDN23 (*ddc1-M8*), and YLDN24 (*ddc1-M11*) were arrested with nocodazole and either UV irradiated (75 J/m²) or mock treated. Protein extracts prepared immediately after UV treatment were separated by SDS-PAGE and analyzed with anti-Ddc1 antibodies.

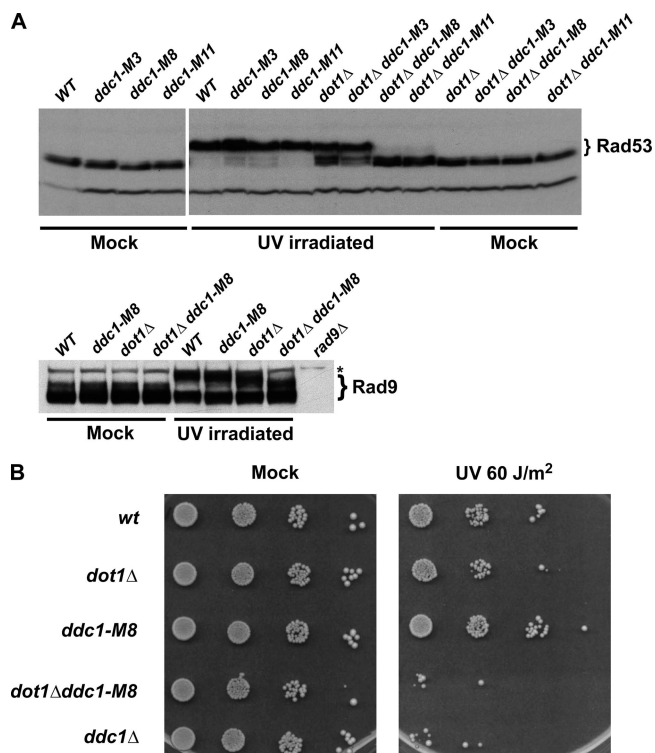


FIG. 4. Phosphorylation of Ddc1 and DOT1 are required for the establishment of an effective UV response. (A) Strains YLDN25 (WT), YLDN17 (*ddc1-M3*), YLDN23 (*ddc1-M8*), YLDN24 (*ddc1-M11*), YFP27 (*dot1Δ*), YFP28 (*dot1Δ ddc1-M3*), YFP29 (*dot1Δ ddc1-M8*), and YFP30 (*dot1Δ ddc1-M11*) were arrested with nocodazole and either UV irradiated (75 J/m²) or mock treated. Rad9 and Rad53 phosphorylations were analyzed 30 min after irradiation. A protein extract from YMIC4E8 (*rad9Δ*) was loaded onto the same gel in order to identify the anti-Rad9 cross-reacting band, indicated by an asterisk. (B) In order to measure sensitivity to UV irradiation, 10-fold serial dilutions of overnight cultures of the strains from panel A and strain YFP152 (*ddc1Δ*) were spotted onto plates, which were then either mock or UV irradiated. Images of the plates were taken after 3 days to assess cell survival.

mutant cell (Fig. 5A and data not shown). To support the hypothesis that the synthetic effect observed when we combined *dot1Δ* with *ddc1-T602A* is due to a loss of Ddc1 phosphorylation, we show that this phenotype is almost completely rescued by a *ddc1-T602S* mutation, which restores a different phosphorylatable residue (Fig. 5B). These observations suggest that Dpb11-mediated recruitment of Rad9 requires Mec1 to phosphorylate Ddc1 on threonine 602. The notion that phosphorylation of Ddc1 on threonine 602 and Dpb11 act in the same pathway is supported by the fact that *ddc1-T602A* and *dpb11-1* are in the same epistasis group for DNA damage-induced Rad53 activation and sensitivity to UV irradiation. In fact, combining the *ddc1-T602A* and *dpb11-1* mutations does not cause defective Rad53 phosphorylation (Fig. 6A). Moreover, the *ddc1-T602A dpb11-1* double mutant is as sensitive to UV irradiation as either single mutant, while a combination of *dot1Δ* with either *ddc1-T602A* or *dpb11-1* is more sensitive than any single mutant and as sensitive as the *dot1Δ ddc1-T602A dpb11-1* triple mutant (Fig. 6B).

Phospho-Ddc1 may be involved in recruiting Dpb11 to the

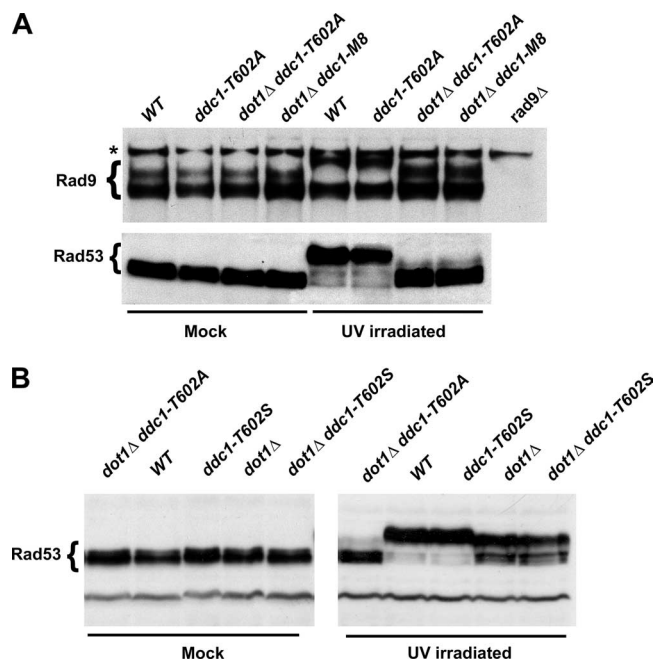


FIG. 5. Phosphorylation of Ddc1 T602 is required for Rad53 and Rad9 phosphorylation in the absence of DOT1. (A) Strains YLDN25 (WT), YLDN9 (*ddc1-T602A*), YFP37 (*dot1Δ ddc1-T602A*), and YFP29 (*dot1Δ ddc1-M8*) were arrested with nocodazole and subjected to UV irradiation (75 J/m²) or mock treated. Rad53 phosphorylation was analyzed 30 min after UV treatment. A protein extract from strain YMIC4E8 (*rad9Δ*) was loaded onto the same gel in order to identify the anti-Rad9 cross-reacting band, indicated by an asterisk. (B) Strains YFP37 (*dot1Δ ddc1-T602A*), YLDN25 (WT), YFP148 (*ddc1-T602S*), YFP27 (*dot1Δ*), and YFP149 (*dot1Δ ddc1-T602S*) were arrested in M phase with nocodazole and either UV irradiated (75 J/m²) or mock treated. Rad53 phosphorylation was analyzed 30 min after treatment.

lesion, bringing it close to the checkpoint kinases. We investigated the possibility that Dpb11 itself may be phosphorylated after DNA damage and whether this may be dependent upon phospho-Ddc1. We used a myc-tagged version of Dpb11 which does not affect cell viability, growth, or genotoxin sensitivity (not shown). After UV irradiation of nocodazole-arrested cells, we detected a modification of Dpb11 which is induced by DNA damage and is dependent upon Mec1 kinase and Ddc1; interestingly, under these experimental conditions, Rad53 also seems to play a partial role in this modification (Fig. 7A). The data presented in Fig. 7A show that in cells with a *ddc1-T602A* phosphorylation site mutation, the DNA damage-induced modification of Dpb11 described above is greatly reduced. The effect of *ddc1-T602A* is even more evident when using a gel that takes advantage of Phos tag technology, which is designed to retard the mobility of phosphorylated proteins (Fig. 7B and C). The defective Dpb11 phosphorylation detected in this mutant background can be explained if phosphorylation of Ddc1-T602 is required to recruit Dpb11 in the vicinity of the lesion.

Consistent with this hypothesis, the interaction between Dpb11 and Ddc1 requires Mec1 activity. The physical interaction between these two factors has been previously shown by using a two-hybrid assay and glutathione *S*-transferase pull-down experiments, while it seems to be undetectable by coimmunoprecipitation (47). We confirmed these findings and

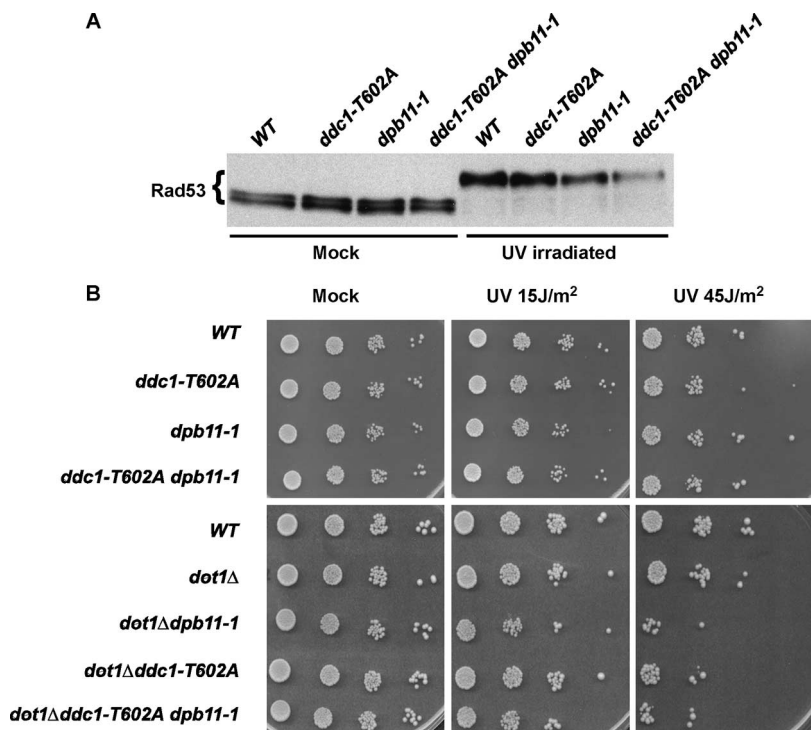


FIG. 6. *ddc1-T602A* and *dpb11-1* mutations are epistatic for UV sensitivity and effect on Rad53 phosphorylation. (A) Strain YFP63 (WT), YFP64 (*ddc1-T602A*), YFP65 (*dpb11-1*), and YFP66 (*dpb11-1 ddc1-T602A*) cells were arrested with nocodazole and UV irradiated. Rad53 phosphorylation was assayed 30 min after treatment. (B) Strains in panel A, YFP27 (*dot1Δ*), YFP142 (*dot1Δ dpb11-1*), YFP37 (*dot1Δ ddc1-T602A*), and YFP144 (*dot1Δ ddc1-T602A dpb11-1*) were grown overnight to stationary phase, and then 10-fold dilutions were spotted onto appropriate plates and either mock treated or UV irradiated with the indicated dosages. Images were taken after 3 days to measure cell survival.

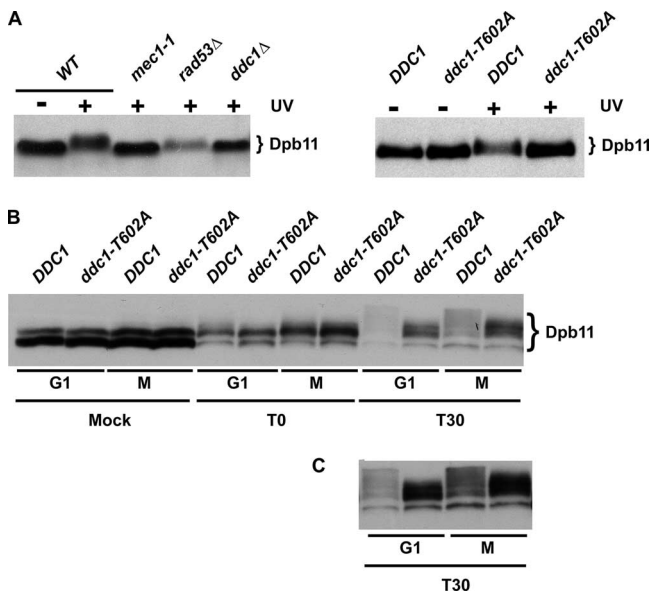


FIG. 7. UV-induced Dpb11 phosphorylation is mediated by Ddc1-T602 and requires Mec1 kinase. (A) Strains YFP38 (WT), YFP48/3a (*mec1-1*), YFP49/1d (*rad53Δ*), YFP55/6c (*ddc1Δ*), YFP63 (*DDC1*), and YFP64 (*ddc1-T602A*), all expressing a myc-tagged Dpb11 protein, were blocked in nocodazole and UV irradiated (75 J/m²). Dpb11 phosphorylation was assessed 30 min after UV irradiation by SDS-PAGE and Western blotting. (B) The indicated strains were arrested in either α -factor (G₁) or nocodazole (M) and UV treated. Protein extracts prepared immediately (T₀) or 30 min (T₃₀) after UV irradiation were separated on Phos tag-conjugated acrylamide gels as described in Materials and Methods. (C) Overexposure of the T₃₀ samples from panel B.

tested whether the interaction between Dpb11 and Ddc1 was dependent upon Mec1 kinase by performing two-hybrid experiments with yeast cells carrying a WT or a *mec1-1* mutant allele and expressing either full-length Ddc1 or a Ddc1 C-terminal fragment (amino acids 309 to 612). Figure 8A shows that a strong positive interaction signal can be detected in WT cells expressing both the full-length and truncated Ddc1 versions; on the other hand, this interaction is lost in a *mec1-1* mutant. When we tried a two-hybrid experiment with a Ddc1-T602A construct, we could not detect any effect on the interaction (not shown). We then tested the interaction between Dpb11 and a Ddc1 mutant (*ddc1-M8*) lacking eight consensus sites for Mec1-dependent phosphorylation. Figure 8B shows that under these conditions, the interaction is greatly reduced, albeit not completely abolished, suggesting that, at least under the experimental conditions of a two-hybrid experiment, there may be some other protein, perhaps Dpb11 itself, that is targeted by Mec1 kinase and plays a role in the interaction between Ddc1 and Dpb11. Another possibility is that, even in the absence of Ddc1 phosphorylation, the highly expressed bait and prey can produce enough hybrid molecules to activate the reporter genes.

As shown in Fig. 1C, a *dpb11-1* temperature-sensitive mutant did not exhibit a significant effect on Ddc2 phosphorylation at permissive temperature. Under these experimental conditions, the Dpb11 protein, albeit missing its C-terminal part, is still present in the cells and is likely to be partially functional. In order to determine whether Dpb11 had a possible role in activating Mec1 kinase, we took advantage of degron technology (49). Briefly, a Dpb11 fu-

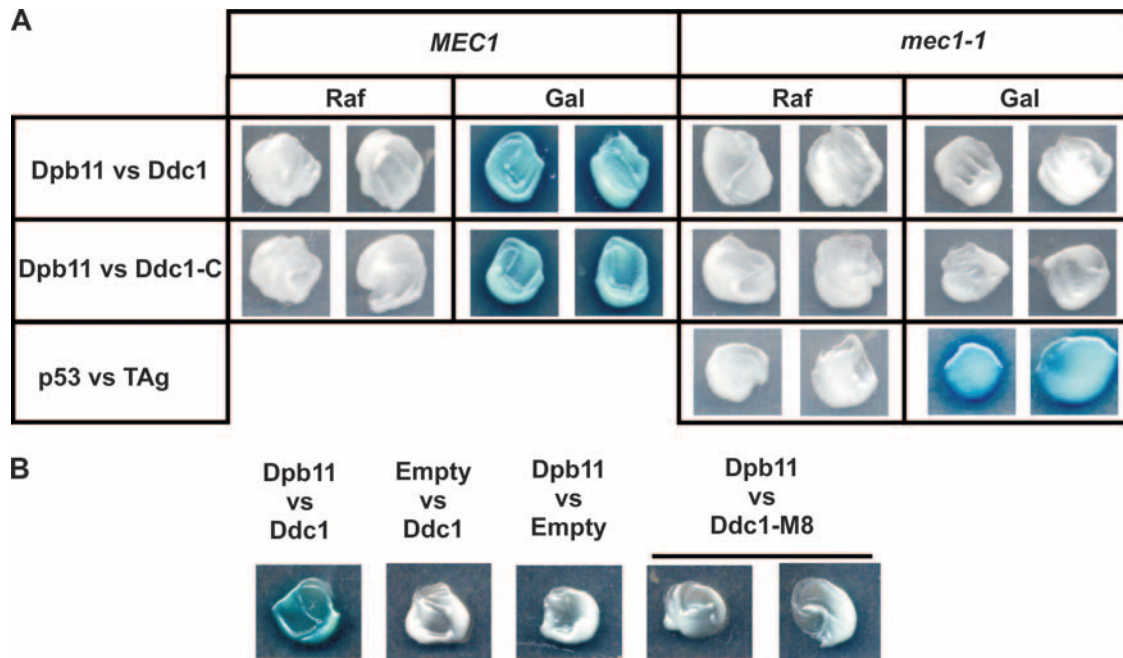


FIG. 8. The interaction between Dpb11 and Ddc1 requires a functional Mec1 kinase. Plasmids pFP1 (pJG4-5-*DPB11*) and pFP2 (pEG202-*DDC1*) were cotransformed with pSH18-34, a β -galactosidase reporter plasmid, in either *MEC1* or *mec1-1* mutant yeast cells. A similar strategy was adopted for pFP4 (pEG202-*ddc1-C*), which carries only the C-terminal fragment (nucleotides 309 to 612) of *DDC1*, containing the 11 putative Mec1 phosphorylation target sites and for pFP10 (pEG202-*ddc1M8*). To assess two-hybrid interaction, these strains were patched onto 5-bromo-4-chloro-3-indolyl- β -D-galactopyranoside (X-Gal) plates containing either raffinose (Raf; Dpb11 prey repressed) or galactose (Gal; Dpb11 prey expressed) as a carbon source. After 3 days, the plates were analyzed. The strains in panel A are YFP50 (*MEC1*, top), YFP52 (*MEC1*, bottom), YFP113 (*mec1-1*, top), and YFP114 (*mec1-1*, bottom). A positive control in the *mec1-1* mutant strain (p53 versus large T antigen [TAg]) was also used. The strains in panel B are, from left to right, YFP50, YFP86, YFP54, and YFP153.

sion protein carrying a temperature-sensitive degron tag (*dpb11^{td}*) is expressed in yeast cells. At 28°C, this construct complements the complete deletion of *DPB11* and does not exhibit any *dpb11*-encoded phenotype (49; data not shown). Once the *dpb11^{td}* culture is shifted to 37°C, the degron tag unfolds and drives the whole fusion protein to rapid degradation via the ubiquitin-mediated pathway (Fig. 9A) (49), allowing us to monitor the effect of a complete loss of the Dpb11 protein. Cells expressing *dpb11^{td}* were grown at 28°C and arrested with nocodazole. Cultures were shifted to 37°C to obtain the complete depletion of Dpb11, shifted back to 28°C, UV irradiated, and analyzed for DNA damage-induced Mec1 activation. Figure 9B shows that depletion of Dpb11 before UV irradiation greatly impairs Mec1-dependent phosphorylation of Ddc2. An isogenic strain, which also expresses WT *DPB11*, responds to UV irradiation with normal Ddc2 phosphorylation. These observations suggest that, after UV irradiation, Dpb11 may also have a more direct function in the robust activation of Mec1, possibly by strengthening its kinase activity, and are supported by similar results obtained with multicellular eukaryotes. A physical interaction between TopBP1 (orthologue of Dpb11) and ATR (orthologue of budding yeast Mec1) has been described in *Xenopus*, and it has been linked to a role for TopBP1 in the checkpoint response, specifically in the activation of ATR itself (21).

DISCUSSION

Loss of genome integrity is a hallmark of cancer cells, and maintenance of genome stability is fundamental to the preven-

tion of tumor development (19). Eukaryotic cells possess a set of complex pathways devoted to monitoring the presence of different kinds of genomic lesions and signaling their presence to downstream effectors. The output of these checkpoint path-

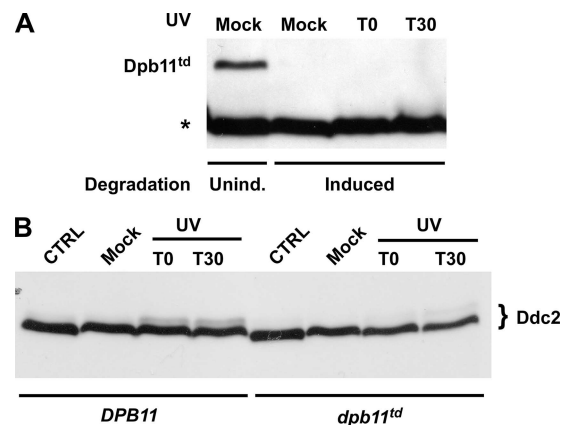


FIG. 9. Dpb11 is required for the full activation of Mec1. (A) Protein extracts from strain YMAG78/4B (*dpb11^{td}*) were prepared under different conditions to assess the presence of the Dpb11-degron protein. Cells were cultured at 28°C in YP plus raffinose (Mock Unind.) and then shifted to the degradation medium at 37°C (Mock Induced), UV irradiated, and shifted back to 25°C (T0, sample taken immediately; T30, sample taken 30 min later). The presence of Dpb11-degron was assessed by using anti-HA antibodies. (B) The experiment was repeated under the same conditions in parallel with strains YMAG82/15a (*DPB11*) and YMAG78/4B (*dpb11^{td}*). Ddc2 hyperphosphorylation was monitored by SDS-PAGE and Western blotting. CTRL, control.

ways is cell cycle arrest, DNA repair, modifications of the transcriptional program, and apoptosis (29, 41). The DNA damage checkpoint pathways are triggered by the activity of apical phosphoinositide 3-like kinases, namely, Mec1 and Tel1 in budding yeast and ATM and ATR in higher eukaryotes. ATM is recruited to DSBs through the Mre11-Rad50-Nbs1 (MRN) complex, while the ATR/ATRIP heterodimer (Mec1/Ddc2 in budding yeast) seems to be recruited by RPA-covered ssDNA filaments generated after nucleolytic processing of damaged DNA (51). The order of function of the players in the checkpoint signal transduction cascade has been defined by monitoring the phosphorylation status of individual proteins. The availability of yeast mutants affected in different factors has greatly aided in this task (5, 25). In budding yeast, once the Mec1 kinase has been brought onto damaged DNA, it phosphorylates a series of targets, among which are Ddc2, the Ddc1 subunit of the 9-1-1 complex, the Rad9 mediator, and the Rad53 downstream kinase (25, 30). Phosphorylation of Rad9, an event that is necessary to relay the signal to the downstream effectors, is strongly influenced by histone modifications. Indeed, monoubiquitination of H2B and methylation of H3 on lysine 79 are required for Rad9 phosphorylation and checkpoint activation in the G₁ phase of the cell cycle, while they have only a partial role in the G₂/M checkpoint response, which in budding yeast arrests the cell cycle in M phase. The mechanism through which histones contribute to Rad9 activation seems to involve the recognition of methylated H3-K79 by the Tudor domain of Rad9, which aids in bringing Rad9 into proximity to the active Mec1 kinase (11, 13, 14, 48). A similar pathway has been described in fission yeast and in higher eukaryotes (4, 7, 16, 39). Given the facts that the G₂/M checkpoint response is still functional in cells lacking Dot1, the histone H3-K79 methyltransferase, and that Rad9 is still highly hyperphosphorylated after UV irradiation of M-phase-arrested cells (11, 48), a parallel, partially redundant pathway leading to the recruitment of Rad9 to damaged chromatin must exist in later stages of the cell cycle. We analyzed in more detail the signaling after UV irradiation of M-phase-arrested *dot1Δ* mutant cells and showed that the residual phosphorylation of Rad9 and Rad53 in these cells is still dependent upon Mec1 kinase and independent of Tel1 or Chk1 checkpoint kinases. One possible mechanism for recruiting Rad9 to damaged chromatin in the absence of H3-K79 methylation could involve the modification of some other histone residues. The analysis of the nucleosomal structure reveals that H3-K79 is in close proximity to H4-K59, and mutation of this residue leads to silencing defects, similarly to mutations in *DOT1* (17, 50). Moreover, in *S. pombe*, Crb2 is recruited through interaction with methylated H4-K20 (39). Our results show that these residues do not seem to be redundant with H3-K79 methylation in the G₂/M checkpoint pathway leading to Rad9 activation; in fact, when mutations in H4-K59 or H4-K20 were combined with *dot1Δ*, we could not detect any synthetic effect on checkpoint activation. We obtained a similarly negative response when we tested strains combining *dot1Δ* with the deletion of the *SET1* or *SET2* histone methyltransferase coding gene. We then tested the contribution of histone H2A phosphorylation on serine 129, which has been shown to be relevant for Rad9 phosphorylation in G₁ cells (14), and we confirmed

that in G₂ this histone modification plays a minor role (14, 18, 46).

Evidence coming from other eukaryotic systems has suggested a role in the DNA damage checkpoint for Dpb11 (Rad4/Cut5 in *S. pombe* and TopBP1 in higher eukaryotes). This factor plays different roles in DNA metabolic processes (reviewed in reference 9), particularly in DNA replication. Recent work showed that TopBP1 in *Xenopus* and mammalian cells can activate the ATR kinase in vitro and this function is mediated by a specific protein domain, which seems to be missing in the fungal orthologues of TopBP1 (15, 21). Moreover, TopBP1 can also interact with the 9-1-1 checkpoint clamp (6, 23). In *S. pombe*, Rad4/Cut5 cooperates in the activation of Chk1 by interacting with the 9-1-1 complex and, in the absence of H2A C-terminal phosphorylation and H4-K20 methylation, it is involved in accumulating the Crb2 mediator at a single persistent DSB. These functions of Rad4/Cut5 are modulated by protein phosphorylation events (7, 8). We combined a *dpb11-1* allele with a deletion of *DOT1* and analyzed the DNA damage checkpoint response after UV irradiation and Zeocin treatment of M-phase-arrested cells. Our results show that, after treatment with UV or induction of DSBs, *dpb11-1* by itself has no major effects on cellular survival; on Ddc2, Rad9, and Rad53 phosphorylation; or on G₂/M checkpoint arrest. On the other hand, when *dpb11-1* is combined with a *dot1Δ* allele, the G₂/M checkpoint is not functional and cells become quite sensitive to UV irradiation and DSB-inducing agents, and the DNA damage-dependent phosphorylation of Rad9 and Rad53 is abolished, while Mec1 activity does not seem to be significantly reduced. These data can be explained if, in the absence of H3-K79 methylation, Rad9 can be recruited through a Dpb11-dependent pathway. Another possible interpretation is that loss of Rad9 phosphorylation may be due to a combination of a reduction of Mec1 kinase activity and a reduction of Rad9 recruitment. In G₁-arrested cells, the importance of Dpb11 for the response to UV is minor; indeed, *dot1Δ* mutant cells cannot arrest at the G₁/S transition and a *dpb11-1* mutation does not worsen this phenotype. Close monitoring of Rad53 phosphorylation in these cells shows that Dpb11 contributes only marginally.

How does Dpb11 mediate Rad9 hyperphosphorylation? In fission yeast, the interaction between the two orthologous factors depends upon the activity of Cdk1 (7), possibly explaining why this pathway is predominant in G₂-M cells. Moreover, Dpb11 contains four BRCT domains and has been reported to interact with the Ddc1 subunit of the 9-1-1 complex (32, 47). In order to investigate the molecular details of this pathway, we analyzed a collection of *DDC1* mutants. Ddc1 sequence analysis revealed the presence of eight consensus sites for Mec1-dependent phosphorylation and three consensus sites for Cdk1-dependent phosphorylation; accordingly, Ddc1 has been reported to be phosphorylated in a cell cycle- and DNA damage-dependent manner (26, 34). We generated a *ddc1-M3* allele lacking the three Cdk1 sites, a *ddc1-M8* version lacking the consensus sites for Mec1 kinase-dependent phosphorylation, and *ddc1-M11*, where all putative phosphorylation sites have been mutated. Both *ddc1-M8* and *ddc1-M11* have lost the DNA damage-dependent phosphorylation of Ddc1. While these mutations, by themselves, do not visibly affect the checkpoint response to DNA damage, when combined with *dot1Δ*,

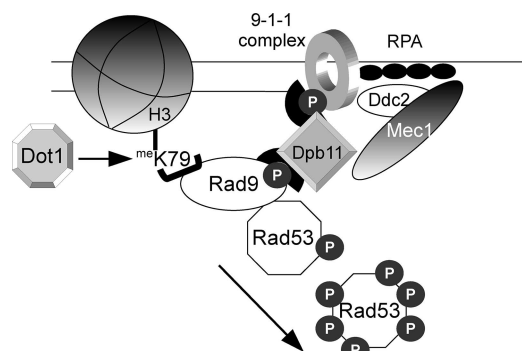


FIG. 10. Possible model of Dpb11 function in the UV-induced DNA damage checkpoint. Dpb11 is recruited to sites of DNA damage through the interaction of its C-terminal BRCTs with the 9-1-1 subunit Ddc1, phosphorylated by Mec1 on T602. Once recruited, it plays a double role in checkpoint activation. First, it enhances Mec1 kinase activity, and second, in G_2/M , it participates with H3-K79 in Rad9 recruitment, likely through an interaction of its N-terminal BRCTs with a Cdc28-phosphorylated site on Rad9. Full Mec1 activity and tight Rad9 recruitment allow rapid and full phosphorylation of Rad53, which correlates with checkpoint activation.

these mutants also eliminate the UV-induced phosphorylation of Rad9 and Rad53 and displayed a synthetic lethality after UV irradiation. This phenotype can be recapitulated by the single *ddc1T602A* mutation and strongly resembles the *dpb11-1*-encoded phenotype described above. Moreover, *ddc1T602A* and *dpb11-1* appear to be in the same epistasis group, which is consistent with the notions that phosphorylation of Ddc1-T602 by Mec1 provides a means to recruit Dpb11 and that the physical interaction between Dpb11 and Ddc1 requires functional Mec1. We showed that Dpb11 is phosphorylated in a DNA damage-dependent and *MEC1*-dependent manner and that this modification appears to be greatly reduced in a *ddc1-T602A* mutant strain, but the functional significance of this modification of Dpb11 is still not clear and will be approached in future work.

The experiments performed with the *dpb11-1* allele did not indicate defective activation of Mec1 kinase following UV damage, in contrast to the *in vitro* data obtained with *Xenopus* and mammalian cell extracts. This could be due to a TopBP1 function which is specific for higher eukaryotes, but recent evidence suggested that an interaction between Rad4/Cut5 and the checkpoint sensor kinase Rad3-Rad26 also exists in *S. pombe* (8, 45). We thus exploited a temperature-sensitive degen version of Dpb11 (*dpb11^{td}*), which can be conditionally eliminated from cells by a combination of transcriptional repression and ubiquitin-dependent degradation (44, 49), to evaluate a possible role for Dpb11 in controlling Mec1 kinase activity *in vivo*. After cells had been depleted of Dpb11 and irradiated with UV light, we detected a noticeable defect in Mec1 activation, as measured by the phosphorylation of its Ddc2 subunit, suggesting that, in budding yeast, Dpb11 can regulate Mec1 by strengthening its kinase activity, even though there is no sequence conservation with the TopBP1 domain required to activate ATR in higher eukaryotes.

Altogether, our data support a model (Fig. 10) in which UV-induced lesions activate the checkpoint cascade to a basal level, likely by bringing Mec1 to damaged DNA via a Ddc2-

RPA interaction; full activation of Mec1 seems to be supported by the presence of Dpb11. Mec1-induced phosphorylation of Ddc1 allows binding of Dpb11, which may cooperate with modified histones in the recruitment of Rad9 to damaged chromatin, allowing signal amplification and a complete response to DNA damage.

ACKNOWLEDGMENTS

We thank D. Gottschling, H. Araki, J. F. X. Diffley, and M. P. Longhese for the gifts of strains and plasmids and C. Santocanale and D. Stern for antibodies. All of the members of the laboratory are acknowledged for stimulating discussion.

This work was supported by grants from the AIRC, the Fondazione Cariplo, the European Union FP6 Integrated Project DNA Repair, and MIUR (to M.M.-F. and P.P.). The financial support of Telethon-Italy (grant GGP030406 to M.M.-F.) is acknowledged.

REFERENCES

- Araki, H., S.-H. Leem, A. Phongdara, and A. Sugino. 1995. Dpb11, which interacts with DNA polymerase II(ϵ) in *Saccharomyces cerevisiae*, has a dual role in S-phase progression and at a cell cycle checkpoint. *Proc. Natl. Acad. Sci. USA* **92**:11791–11795.
- Bakkenist, C. J., and M. B. Kastan. 2004. Initiating cellular stress responses. *Cell* **118**:9–17.
- Bartek, J., and N. Mailand. 2006. TOPping up ATR activity. *Cell* **124**:888–890.
- Botuyan, M. V., J. Lee, I. M. Ward, J. E. Kim, J. R. Thompson, J. Chen, and G. Mer. 2006. Structural basis for the methylation state-specific recognition of histone H4-K20 by 53BP1 and Crb2 in DNA repair. *Cell* **127**:1361–1373.
- Carr, A. M. 2002. DNA structure dependent checkpoints as regulators of DNA repair. *DNA Repair* **1**:983–994.
- Delacroix, S., J. M. Wagner, M. Kobayashi, K. Yamamoto, and L. M. Karnitz. 2007. The Rad9-Hus1-Rad1 (9-1-1) clamp activates checkpoint signaling via TopBP1. *Genes Dev.* **21**:1472–1477.
- Du, L. L., T. M. Nakamura, and P. Russell. 2006. Histone modification-dependent and -independent pathways for recruitment of checkpoint protein Crb2 to double-strand breaks. *Genes Dev.* **20**:1583–1596.
- Furuya, K., M. Poitelea, L. Guo, T. Caspari, and A. M. Carr. 2004. Chk1 activation requires Rad9 S/TQ-site phosphorylation to promote association with C-terminal BRCT domains of Rad4TOPBP1. *Genes Dev.* **18**:1154–1164.
- Garcia, V., K. Furuya, and A. M. Carr. 2005. Identification and functional analysis of TopBP1 and its homologs. *DNA Repair* **4**:1227–1239.
- Giannattasio, M., F. Lazzaro, M. P. Longhese, P. Plevani, and M. Muzi-Falconi. 2004. Physical and functional interactions between nucleotide excision repair and DNA damage checkpoint. *EMBO J.* **23**:429–438.
- Giannattasio, M., F. Lazzaro, P. Plevani, and M. Muzi-Falconi. 2005. The DNA damage checkpoint response requires histone H2B ubiquitination by Rad6-Bre1 and H3 methylation by Dot1. *J. Biol. Chem.* **280**:9879–9886.
- Gilbert, C. S., C. M. Green, and N. F. Lowndes. 2001. Budding yeast Rad9 is an ATP-dependent Rad53 activating machine. *Mol. Cell* **8**:129–136.
- Grenon, M., T. Costelloe, S. Jimeno, A. O'Shaughnessy, J. Fitzgerald, O. Zgheib, L. Degerth, and N. F. Lowndes. 2007. Docking onto chromatin via the *Saccharomyces cerevisiae* Rad9 Tudor domain. *Yeast* **24**:105–119.
- Hammet, A., C. Magill, J. Heierhorst, and S. P. Jackson. 2007. Rad9 BRCT domain interaction with phosphorylated H2AX regulates the G_1 checkpoint in budding yeast. *EMBO Rep.* **8**:851–857.
- Hashimoto, Y., T. Tsujimura, A. Sugino, and H. Takisawa. 2006. The phosphorylated C-terminal domain of *Xenopus* Cut5 directly mediates ATR-dependent activation of Chk1. *Genes Cells* **11**:993–1007.
- Huyen, Y., O. Zgheib, R. A. Ditullio, Jr., V. G. Gorgoulis, P. Zacharatos, T. J. Petty, E. A. Shestov, H. S. Mellert, E. S. Stavridi, and T. D. Halazonetis. 2004. Methylated lysine 79 of histone H3 targets 53BP1 to DNA double-strand breaks. *Nature* **432**:406–411.
- Hyland, E. M., M. S. Cosgrove, H. Molina, D. Wang, A. Pandey, R. J. Cottee, and J. D. Boeke. 2005. Insights into the role of histone H3 and histone H4 core modifiable residues in *Saccharomyces cerevisiae*. *Mol. Cell. Biol.* **25**:10060–10070.
- Javaheri, A., R. Wysocki, O. Jobin-Robitaille, M. Altaf, J. Cote, and S. J. Kron. 2006. Yeast G_1 DNA damage checkpoint regulation by H2A phosphorylation is independent of chromatin remodeling. *Proc. Natl. Acad. Sci. USA* **103**:13771–13776.
- Kastan, M. B., and J. Bartek. 2004. Cell-cycle checkpoints and cancer. *Nature* **432**:316–323.
- Kelly, T. J., S. Qin, D. E. Gottschling, and M. R. Parthun. 2000. Type B histone acetyltransferase Hat1p participates in telomeric silencing. *Mol. Cell. Biol.* **20**:7051–7058.

21. Kumagai, A., J. Lee, H. Y. Yoo, and W. G. Dunphy. 2006. TopBP1 activates the ATR-ATRIP complex. *Cell* **124**:943–955.
22. Lachner, M., and T. Jenuwein. 2002. The many faces of histone lysine methylation. *Curr. Opin. Cell Biol.* **14**:286–298.
23. Lee, J., A. Kumagai, and W. G. Dunphy. 2007. The Rad9-Hus1-Rad1 checkpoint clamp regulates interaction of TopBP1 with ATR. *J. Biol. Chem.* **282**:28036–28044.
24. Lisby, M., J. H. Barlow, R. C. Burgess, and R. Rothstein. 2004. Choreography of the DNA damage response: spatiotemporal relationships among checkpoint and repair proteins. *Cell* **118**:699–713.
25. Longhese, M. P., M. Foiani, M. Muzi-Falconi, G. Lucchini, and P. Plevani. 1998. DNA damage checkpoint in budding yeast. *EMBO J.* **17**:5525–5528.
26. Longhese, M. P., V. Paciotti, R. Fraschini, R. Zaccarini, P. Plevani, and G. Lucchini. 1997. The novel DNA damage checkpoint protein Ddc1p is phosphorylated periodically during the cell cycle and in response to DNA damage in budding yeast. *EMBO J.* **16**:5216–5226.
27. Longtine, M. S., A. McKenzie III, D. J. Demarini, N. G. Shah, A. Wach, A. Brachat, P. Philippsen, and J. R. Pringle. 1998. Additional modules for versatile and economical PCR-based gene deletion and modification in *Saccharomyces cerevisiae*. *Yeast* **14**:953–961.
28. Majka, J., and P. M. Burgers. 2003. Yeast Rad17/Mec3/Ddc1: a sliding clamp for the DNA damage checkpoint. *Proc. Natl. Acad. Sci. USA* **100**:2249–2254.
29. McGowan, C. H., and P. Russell. 2004. The DNA damage response: sensing and signaling. *Curr. Opin. Cell Biol.* **16**:629–633.
30. Melo, J., and D. Toczyski. 2002. A unified view of the DNA-damage checkpoint. *Curr. Opin. Cell Biol.* **14**:237–245.
31. Muzi-Falconi, M., A. Piseri, M. Ferrari, G. Lucchini, P. Plevani, and M. Foiani. 1993. *De novo* synthesis of budding yeast DNA polymerase α and *POL1* transcription at the G₁/S boundary are not required for entrance into S phase. *Proc. Natl. Acad. Sci. USA* **90**:10519–10523.
32. Ogiwara, H., A. Ui, F. Onoda, S. Tada, T. Enomoto, and M. Seki. 2006. Dpb11, the budding yeast homolog of TopBP1, functions with the checkpoint clamp in recombination repair. *Nucleic Acids Res.* **34**:3389–3398.
33. Paciotti, V., M. Clerici, G. Lucchini, and M. P. Longhese. 2000. The checkpoint protein Ddc2, functionally related to *S. pombe* Rad26, interacts with Mec1 and is regulated by Mec1-dependent phosphorylation in budding yeast. *Genes Dev.* **14**:2046–2059.
34. Paciotti, V., G. Lucchini, P. Plevani, and M. P. Longhese. 1998. Mec1p is essential for phosphorylation of the yeast DNA damage checkpoint protein Ddc1p, which physically interacts with Mec3p. *EMBO J.* **17**:4199–4209.
35. Parrilla-Castellar, E. R., and L. M. Karnitz. 2003. Cut5 is required for the binding of Atr and DNA polymerase α to genotoxin-damaged chromatin. *J. Biol. Chem.* **278**:45507–45511.
36. Pelliccioli, A., C. Lucca, G. Liberi, F. Marini, M. Lopes, P. Plevani, A. Romano, P. P. Di Fiore, and M. Foiani. 1999. Activation of Rad53 kinase in response to DNA damage and its effect in modulating phosphorylation of the lagging strand DNA polymerase. *EMBO J.* **18**:6561–6572.
37. Rouse, J., and S. P. Jackson. 2000. *LCD1*: an essential gene involved in checkpoint control and regulation of the *MEC1* signalling pathway in *Saccharomyces cerevisiae*. *EMBO J.* **19**:5801–5812.
38. Rouse, J., and S. P. Jackson. 2002. Lcd1p recruits Mec1p to DNA lesions in vitro and in vivo. *Mol. Cell* **9**:857–869.
39. Sanders, S. L., M. Portoso, J. Mata, J. Bahler, R. C. Allshire, and T. Kouzarides. 2004. Methylation of histone H4 lysine 20 controls recruitment of Crb2 to sites of DNA damage. *Cell* **119**:603–614.
40. Schwartz, M. F., J. K. Duong, Z. Sun, J. S. Morrow, D. Pradhan, and D. F. Stern. 2002. Rad9 phosphorylation sites couple Rad53 to the *Saccharomyces cerevisiae* DNA damage checkpoint. *Mol. Cell* **9**:1055–1065.
41. Shiloh, Y. 2003. ATM and related protein kinases: safeguarding genome integrity. *Nat. Rev. Cancer* **3**:155–168.
42. Shiloh, Y. 2006. The ATM-mediated DNA-damage response: taking shape. *Trends Biochem. Sci.* **31**:402–410.
43. Sun, Z. X., J. Hsiao, D. S. Fay, and D. F. Stern. 1998. Rad53 Fha domain associated with phosphorylated Rad9 in the DNA damage checkpoint. *Science* **281**:272–274.
44. Tanaka, S., and J. F. X. Diffley. 2002. Interdependent nuclear accumulation of budding yeast Cdt1 and Mcm2-7 during G₁ phase. *Nat. Cell Biol.* **4**:198–207.
45. Taricani, L., and T. S. Wang. 2006. Rad4TopBP1, a scaffold protein, plays separate roles in DNA damage and replication checkpoints and DNA replication. *Mol. Biol. Cell* **17**:3456–3468.
46. Toh, G. W., A. M. O'Shaughnessy, S. Jimeno, I. M. Dobbie, M. Grenon, S. Maffini, A. O'Rourke, and N. F. Lowndes. 2006. Histone H2A phosphorylation and H3 methylation are required for a novel Rad9 DSB repair function following checkpoint activation. *DNA Repair* **5**:693–703.
47. Wang, H., and S. J. Elledge. 2002. Genetic and physical interactions between DPB11 and DDC1 in the yeast DNA damage response pathway. *Genetics* **160**:1295–1304.
48. Wysocki, R., A. Javaheri, S. Allard, F. Sha, J. Cote, and S. J. Kron. 2005. Role of Dot1-dependent histone H3 methylation in G₁ and S phase DNA damage checkpoint functions of Rad9. *Mol. Cell. Biol.* **25**:8430–8443.
49. Zegerman, P., and J. F. X. Diffley. 2007. Phosphorylation of Sld2 and Sld3 by cyclin-dependent kinases promotes DNA replication in budding yeast. *Nature* **445**:281–285.
50. Zhang, L., E. E. Eugeni, M. R. Parthun, and M. A. Freitas. 2003. Identification of novel histone posttranslational modifications by peptide mass fingerprinting. *Chromosoma* **112**:77–86.
51. Zou, L., and S. J. Elledge. 2003. Sensing DNA damage through ATRIP recognition of RPA-ssDNA complexes. *Science* **300**:1542–1548.